Inorganic Chemistry

Article

pubs.acs.org/IC

High-Temperature, High-Pressure Hydrothermal Synthesis, Crystal Structures, and Spectroscopic Studies of a Uranium(IV) Phosphate ($Na_{10}U_2P_6O_{24}$) and the Isotypic Cerium(IV) Phosphate ($Na_{10}Ce_2P_6O_{24}$)

Yu-Hsien Lai,[†] Yu-Chih Chang,[†] Tsz-Fung Wong,[‡] Wan-Ju Tai,[†] Wen-Jung Chang,[†] and Kwang-Hwa Lii*[,†,§]

[†]Department of Chemistry, National Central University, Jhongli, Taiwan 320, R.O.C.

[‡]Department of Chemistry, The Chinese University of Hong Kong, Shatin, New Territories, Hong Kong

[§]Institute of Chemistry, Academia Sinica, Taipei, Taiwan 115, R.O.C.

Supporting Information

ABSTRACT: A uranium(IV) phosphate, $Na_{10}U_2P_6O_{24}$, was synthesized under hydrothermal conditions at 570 °C and 160 MPa and structurally characterized by single-crystal X-ray diffraction. The valence state of uranium was established by UV−vis and U 4f X-ray photoelectron spectroscopy. The powder sample has a second-harmonic-generation signal, confirming the absence of a center of symmetry in the structure. The structure contains UO_8 snub-disphenoidal polyhedra that are linked to monophosphate tetrahedra by vertex and edge sharing such that a three-dimensional framework with intersecting 12-sided circular and rectangular channels is formed. All 10 sodium sites are situated inside the channels and are fully occupied. This is the first uranium(IV) phosphate synthesized under high-temperature, high-pressure hydrothermal conditions. The isotypic cerium(IV) phosphate, $Na_{10}Ce_2P_6O_{24}$, was also synthesized under the same hydrothermal conditions. It is the first structurally characterized Ce(IV) phosphate with a P/Ce ratio of 3. Crystal data of $Na_{10}U_2P_6O_{24}$: orthorhombic, $P2_12_12_1$ (No. 19), a = 6.9289(3) Å, b = 16.1850(7) Å, c = 18.7285(7) Å, V = 2100.3(2) Å^3, Z = 4, R_1 = 0.0304, and wR_2 = 0.0522. Crystal data of $Na_{10}Ce_2P_6O_{24}$: orthorhombic, $P2_12_12_1$ (No. 19), a = 6.9375(14) Å, b = 16.215(3) Å, c = 18.765(4) Å, V = 2111.0(7) Å^3, Z = 4, R_1 = 0.0202, and wR_2 = 0.0529.

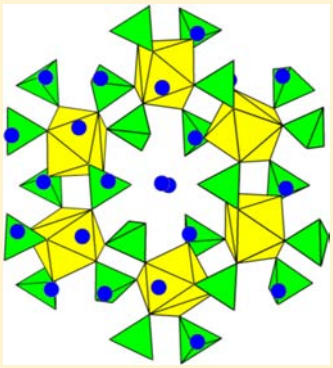

INTRODUCTION

Although uranium exhibits oxidation states from +3 to +6, only uranium(IV) and uranium(VI) are important in minerals. When the U^{6+} cation is coordinated by seven or eight oxygen atoms, it is almost always present as part of a uranyl ion, UO_2^{2+}, which is linear or nearly so. However, when the U^{6+} cation is coordinated by six oxygen atoms, considerable bond length variability is observed.[1] Dissolved UO_2^{2+}, which is derived from the oxidative dissolution of U-bearing minerals, reacts with oxyanions to form relatively insoluble uranyl oxysalt minerals such as uranyl silicates, phosphates, vanadates, arsenates, and molybdates.[2] Uranyl silicates are the most abundant group of uranyl minerals in many instances, and in addition, a large number of synthetic uranyl silicates have been reported.[3] In contrast to uranyl silicate minerals, only two naturally occurring uranium(IV) silicates, namely, coffinite, $USiO_4$, and arapovite, $U^{4+}(Ca,Na)_2(K_{1-x}\square_x)[Si_8O_{22}]$ (□ denotes vacancy), were discovered.[4,5] The structure of coffinite was reported for a synthetic crystal to be a tetragonal orthosilicate isostructural with zircon, $ZrSiO_4$. A uranium(IV) germanate, $UGeO_4$, has been synthesized by a solid-state reaction.[6] Recently, we reported the first synthetic U(IV) silicate, $Cs_2USi_6O_{15}$, whose structure is closely related to that of $Cs_2ThSi_6O_{15}$ and those of several neodymium and zirconium silicates and germanates.[7] A U(IV) germanate, $Cs_4UGe_8O_{20}$, that adopts a new structure and contains four- and five-coordinate germanium was also synthesized under high-temperature, high-pressure hydrothermal conditions.[8]

Uranium phosphate species are also among the most numerous, widespread, abundant, and insoluble actinide-bearing materials and, therefore, have been studied as potential actinide host phases.[9] Therefore, the synthesis and crystal chemistry of uranium phosphates have been subjects of intense interest because the structures and behaviors of these compounds provide a basis from which to predict the long-term behavior of actinide-bearing phosphates. Few tetravalent uranium silicates are known; by contrast, a large number of uranium(IV) phosphates have been reported.[10] This is because the phosphate materials can form in acidic solutions and the reduction of uranium from U^{VI} to U^{IV} occurs more readily at lower pH.[11] Recently, we have extended the exploratory synthetic and structural studies to the class of uranium phosphates and obtained a new tetravalent uranium phosphate, $Na_{10}U_2P_6O_{24}$ (further denoted as **1**), under hydrothermal conditions at 570 °C and 160 MPa. This is the first

Received: August 29, 2013
Published: November 13, 2013

   dx.doi.org/10.1021/ic402208s | *Inorg. Chem.* 2013, 52, 13639−13643

uranium(IV) phosphate synthesized under high-temperature, high-pressure hydrothermal conditions. We report the synthesis, single-crystal X-ray structure, and spectroscopic studies of **1**.

Structures of some tetravalent actinide compounds are isotypic with their tetravalent rare earth analogues. Cerium(IV) phosphates (CePs) are of interest because some of them exhibit properties such as cation exchange, proton conductivity, trapping of radioactive elements, and amine interaction.[12,13] Compared with Zr, Ti, and Sn phosphates, which are well-documented materials, CePs appear to be much more complex. Many of these CePs structures have remained unknown. The first structures of CePs with P/Ce ratios of 1.5/1 and 2/1, $Ce(PO_4)(HPO_4)_{0.5}(H_2O)_{0.5}$ and $(NH_4)_2Ce(PO_4)_2{\cdot}H_2O$, respectively, have only recently been determined by powder X-ray diffraction.[12,13] Therefore, we conducted hydrothermal crystal growth of the Ce(IV) phosphate $Na_{10}Ce_2P_6O_{24}$ (further denoted as **2**). To the best of our knowledge, **2** is the first structurally characterized Ce(IV) phosphate with a P/Ce ratio of 3.

EXPERIMENTAL SECTION

Synthesis and Initial Characterization. High-temperature, high-pressure hydrothermal synthesis was performed in gold ampules contained in a Leco Tem-Pres autoclave where the pressure was provided by water. A reaction mixture of 259 μL of 10 M NaOH(aq), 13.6 mg of NaF, 30.9 mg of UO_3, 3.5 mg of Zn, and 297.2 mg of NaH_2PO_4 (39/1/0.5/12 Na/U/Zn/P molar ratio) sealed in a 4.1 cm gold ampule (inside diameter of 0.48 cm) was placed in an autoclave and counterpressured with water at a fill level of 55%. Zinc metal was included in the reaction mixture as a reducing agent. The autoclave was heated at 570 °C for 2 days, cooled to 350 °C at a rate of 5 °C/h, and then quenched to room temperature by being removed from the furnace. The pressure at 570 °C was estimated to be 160 MPa according to the $P-T$ diagram of pure water. The product was filtered off, washed with water, rinsed with ethanol, and dried at ambient temperature in a desiccator. The reaction produced green needle crystals of **1** as the major phase together with some colorless crystals of unidentified materials. A qualitative energy-dispersive X-ray (EDX) analysis of several green crystals did not reveal any Zn or F and confirmed the presence of Na, U, and P. A suitable crystal was selected for single-crystal X-ray diffraction, from which the chemical formula was determined. The green crystals were manually separated from the others, giving a pure sample as indicated by powder X-ray diffraction (Figure S1 of the Supporting Information). The yield of **1** was 57.3% based on uranium. For comparison, a hydrothermal reaction at 400 °C was also performed. We were unable to characterize the polycrystalline product by powder X-ray diffraction. Attempts to synthesize the potassium analogue of **1** have been unsuccessful.

A reaction mixture of 219.1 μL of 10 M NaOH(aq), 23.0 mg of NaF, 31.4 mg of CeO_2, and 262.9 mg of NaH_2PO_4 (27/1/12 Na/Ce/P molar ratio) sealed in a 4.3 cm gold ampule (inside diameter of 0.48 cm) was placed in an autoclave and counterpressured with water at a fill level of 55%. The autoclave was heated at 570 °C for 2 days, cooled to 350 °C at a rate of 5 °C/h, and then quenched to room temperature by being removed from the furnace. The reaction produced pale yellow needle crystals of **2** as the major phase together with some colorless wedge-shaped crystals. The latter crystal does not contain phosphorus and has not been identified because of twinning. A needle crystal was selected for single-crystal X-ray diffraction. The needle crystals could be manually separated from the others, giving a pure sample as indicated by powder X-ray diffraction (Figure S2 of the Supporting Information). A pure product of **2** was prepared under the same hydrothermal reaction conditions except that some $NaNO_3$ ($NaNO_3/CeO_2$ molar ratio of 0.5) was included in the reaction mixture to prevent the formation of the Ce(III) compound. The yield was 80.7% based on cerium. For comparison, a hydrothermal reaction at 400 °C was also performed. The polycrystalline product contained **2** and an unidentified phase.

UV−vis data were acquired from a pressed pellet of an intimate mixture of **1** and KBr at room temperature using a Hitachi U-4100 spectrophotometer.

Single-Crystal X-ray Diffraction. A green crystal of **1** with dimensions of 0.48 mm × 0.08 mm × 0.08 mm (Figure S2 of the Supporting Information) was selected for indexing and intensity data collection on a Bruker Kappa Apex II CCD diffractometer equipped with a normal focus, 3 kW sealed tube X-ray source. Intensity data were collected at 296 K over 1319 frames with φ and ω scans (width of 0.5°/frame) and an exposure time of 10 s/frame. Determination of integrated intensities and unit cell refinement were performed using SAINT.[14] SADABS was used for absorption correction (T_{min}/T_{max} = 0.472/0.746).[15] On the basis of statistical analysis of the intensity distribution and successful solution and refinement of the structure, the space group was determined to be $P2_12_12_1$ (No. 19). The structure was determined by direct methods and successive difference Fourier synthesis. Ten Na atom sites were located and refined with full occupancy. The final cycles of least-squares refinement, including atomic coordinates and anisotropic thermal parameters for all atoms, converged at R_1 = 0.0304, wR_2 = 0.0522 for 4716 reflections with $I > 2\sigma(I)$, GooF = 1.045, $\rho_{max,min}$ = 2.26, and −1.34 e Å^{-3}. All calculations were performed using SHELXTL version 6.14.[16]

A colorless crystal of **2** with dimensions of 0.57 mm × 0.07 mm × 0.07 mm (Figure S4 of the Supporting Information) was selected for indexing and intensity data collection. The crystal was found to be a two-component nonmerohedral twin. The integration of collected data using an orthorhombic unit cell yielded a total of 3597 independent reflections to a maximal θ angle of 28.39°, of which 3526 (98.0%) were greater than $2\sigma(F^2)$. TWINABS based on multiple scanned reflections was used for absorption correction.[17] The structure was determined from a detwinned HKLF 4 reflection file using *cell_now*[18] and refined by full-matrix least-squares refinement on F^2 with SHELXL-97 using the HKLF 5 option. An additional variable using the BASF instruction that describes the fractional contributions of twin components was introduced. All atoms were refined with anisotropic displacement parameters: T_{min}/T_{max} = 0.568/0.746, R_1 = 0.0202, wR_2 = 0.0529 for 3526 reflections with $I > 2\sigma(I)$, GooF = 1.072, $\rho_{max,min}$ = 0.70, and −0.75 e Å^{-3}. The crystallographic data are listed in Table 1 and selected bond distances in Table 2.

Because SHG provides a highly sensitive and definite test of the absence of a center of symmetry of crystalline materials, the SHG

Table 1. Crystallographic Data for $Na_{10}U_2P_6O_{24}$ (1) and $Na_{10}Ce_2P_6O_{24}$ (2)

	1	2
chemical formula	$Na_{10}O_{24}P_6U_2$	$Ce_2Na_{10}O_{24}P_6$
formula weight	1275.78	1079.96
crystal system	orthorhombic	orthorhombic
space group	$P2_12_12_1$ (No. 19)	$P2_12_12_1$ (No. 19)
a (Å)	6.9289(3)	6.9375(14)
b (Å)	16.1850(7)	16.215(3)
c (Å)	18.7285(7)	18.765(4)
V (Å^3)	2100.3(2)	2111.0(7)
Z	4	4
T (°C)	23	23
λ(Mo Kα) (Å)	0.71073	0.71073
D_{calc} (g cm^{-3})	4.035	3.398
μ(Mo Kα) (mm^{-1})	16.19	50.4
$R_1{}^a$	0.0304	0.0202
$wR_2{}^b$	0.0522	0.0529

$^aR_1 = \sum||F_o| - |F_c||/\sum|F_o|$. $^bwR_2 = [\sum w(F_o^2 - F_c^2)^2/\sum w(F_o^2)^2]^{1/2}$, where $w = 1/[\sigma^2(F_o^2) + (aP)^2 + bP]$, where $P = [\max(F_o^2,0) + 2(F_c)^2]/3$, where a = 0.023 and b = 0 for **1** and a = 0.0231 and b = 5.62 for **2**.

dx.doi.org/10.1021/ic402208s | *Inorg. Chem.* 2013, 52, 13639−13643

Table 2. Selected Bond Lengths (angstroms) for $Na_{10}U_2P_6O_{24}$ (1) and $Na_{10}Ce_2P_6O_{24}$ (2)[a]

Compound 1			
U(1)–O(1)	2.450(4)	U(1)–O(4)	2.460(5)
U(1)–O(5)	2.444(5)	U(1)–O(8)	2.385(4)
U(1)–O(12)	2.446(5)	U(1)–O(16)	2.324(5)
U(1)–O(19)	2.310(5)	U(1)–O(20)	2.214(5)
U(2)–O(2)	2.349(4)	U(2)–O(7)	2.354(5)
U(2)–O(10)	2.438(5)	U(2)–O(11)	2.442(4)
U(2)–O(14)	2.353(4)	U(2)–O(15)	2.563(5)
U(2)–O(21)	2.328(4)	U(2)–O(24)	2.216(5)
P(1)–O(1)	1.549(6)	P(1)–O(2)	1.536(4)
P(1)–O(3)	1.510(5)	P(1)–O(4)	1.539(5)
P(2)–O(5)	1.549(5)	P(2)–O(6)	1.505(5)
P(2)–O(7)	1.536(5)	P(2)–O(8)	1.540(5)
P(3)–O(9)	1.516(5)	P(3)–O(10)	1.550(5)
P(3)–O(11)	1.540(5)	P(3)–O(12)	1.537(5)
P(4)–O(13)	1.507(4)	P(4)–O(14)	1.548(5)
P(4)–O(15)	1.537(5)	P(4)–O(16)	1.538(5)
P(5)–O(17)	1.498(5)	P(5)–O(18)	1.510(5)
P(5)–O(19)	1.537(5)	P(5)–O(20)	1.567(5)
P(6)–O(21)	1.556(5)	P(6)–O(22)	1.511(5)
P(6)–O(23)	1.499(5)	P(6)–O(24)	1.564(5)
Compound 2			
Ce(1)–O(1)	2.390(4)	Ce(1)–O(4)	2.456(4)
Ce(1)–O(5)	2.446(4)	Ce(1)–O(8)	2.347(3)
Ce(1)–O(12)	2.444(4)	Ce(1)–O(16)	2.308(4)
Ce(1)–O(19)	2.298(4)	Ce(1)–O(20)	2.208(4)
Ce(2)–O(2)	2.352(4)	Ce(2)–O(7)	2.342(4)
Ce(2)–O(10)	2.445(4)	Ce(2)–O(11)	2.395(4)
Ce(2)–O(14)	2.312(4)	Ce(2)–O(15)	2.538(4)
Ce(2)–O(21)	2.322(4)	Ce(2)–O(24)	2.196(4)
P(1)–O(1)	1.548(4)	P(1)–O(2)	1.553(4)
P(1)–O(3)	1.511(4)	P(1)–O(4)	1.556(4)
P(2)–O(5)	1.556(4)	P(2)–O(6)	1.514(4)
P(2)–O(7)	1.549(4)	P(2)–O(8)	1.540(4)
P(3)–O(9)	1.521(4)	P(3)–O(10)	1.560(4)
P(3)–O(11)	1.544(5)	P(3)–O(12)	1.555(4)
P(4)–O(13)	1.510(4)	P(4)–O(14)	1.551(5)
P(4)–O(15)	1.547(4)	P(4)–O(16)	1.552(4)
P(5)–O(17)	1.513(4)	P(5)–O(18)	1.514(4)
P(5)–O(19)	1.556(4)	P(5)–O(20)	1.570(4)
P(6)–O(21)	1.565(4)	P(6)–O(22)	1.519(4)
P(6)–O(23)	1.509(4)	P(6)–O(24)	1.574(4)

[a]The Na–O distances are available in the Supporting Information.

responses of powder samples of **1** and **2** were measured.[19] When the powder sample was exposed to the fundamental output (1064 nm) of a pulsed Nd:YAG laser, a weak but definite green emission generated from the sample could be detected, confirming the absence of a center of symmetry in the structures of both compounds (Figures S3 and S4 of the Supporting Information).

X-ray Photoelectron Spectroscopy. The XPS data of a crystal of **1** were recorded on a PHI Quantera SXM spectrometer using monochromatic Al Kα (1486.6 eV) X-ray radiation at room temperature. The anode was operated at 24.2 W with a typical spot size of 100 μm. The sample was etched using a 1 kV Ar^+ ion beam for 5 s before measurement. The binding energy scale was referenced to adventitious C 1s at 285.0 eV. The U 4f data were analyzed with MultiPak software using the iterated Shirley background and the asymmetric peak profile for both primary and satellite peaks. The fitting parameters of the XPS data are given in Table S1 of the Supporting Information.

RESULTS AND DISCUSSION

Structures. The structure of **1** consists of the following distinctly different structural elements: two UO_8 polyhedra, six monophosphate tetrahedra, and 10 Na sites. Both uranium atoms are bonded by eight oxygen atoms at distances ranging from 2.214 to 2.460 Å for $U(1)O_8$ and from 2.216 to 2.563 Å for $U(2)O_8$. These two polyhedra do not contain a UO_2^{2+} cation. The average U–O bond lengths are 2.379 and 2.380 Å for $U(1)O_8$ and $U(2)O_8$, respectively, which are close to the predicted value of 2.35 Å for the U^{4+}–O bond according to the effective ionic radius for an eight-coordinate U^{4+} ion.[20] Bond valence sums were used to correlate the crystal structure analysis results and oxidation states. Using the parameters from Brese and O'Keeffe, R_o = 2.112 Å and b = 0.37 Å,[21] the bond valence sums at U(1) and U(2) sites are 3.99 and 4.00 valence units, respectively, consistent with the presence of U^{4+} ions at these sites. These UO_8 polyhedra correspond to a snub disphenoid that has 12 triangular faces. This triangular dodecahedron is not a regular polyhedron because some vertices have four faces and others have five. The U^{4+} cations occur in several recently reported uranium(IV) silicates and germanates in regular octahedral coordination, in contrast to the dodecahedron in **1**. For example, the UO_6 octahedron in the silicate $Cs_2USi_6O_{15}$ is regular with d(U–O) in the range from 2.209(6) to 2.256(4) Å.[7] The U–O bond lengths in the UO_6 octahedron in the germanate $Cs_4UGe_8O_{20}$ are in the range from 2.197(3) to 2.277(3) Å.[8] The phosphate tetrahedron is smaller in size than that of silicate, and the oxygen atom receives more bond valence from phosphorus than from silicon. Thus, the coordination number of U^{4+} in phosphate tends to be larger than that in silicate. This is in agreement with the observation that in contrast to the relative paucity of phosphate structures with the tetravalent actinides in 6- or 7-fold coordination, 8-fold coordination is shown by at least six different structure types.[20] Both U(1) and U(2) in the structure of **1** are joined to four phosphate groups by vertex sharing and with two phosphate groups by edge sharing (Figure 1). Each U atom is connected to three U atoms through phosphate groups to form a three-dimensional framework with intersecting 12-sided circular and rectangular channels along the a and b axes, respectively (Figure 2). Columns with the 12-membered circular window are closely packed in space. The rectangular channel is narrow with a width of only one UO_8 polyhedron

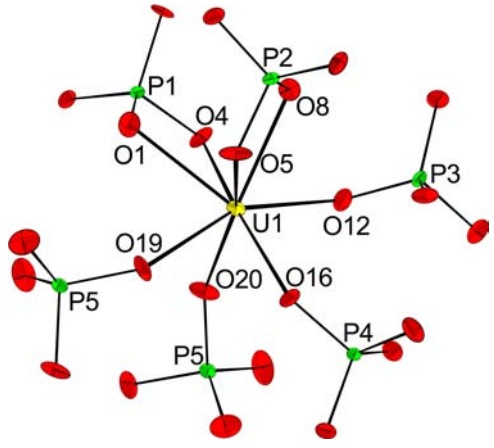

Figure 1. Coordination environments of U(1) in **1** showing the atom labeling scheme. Thermal ellipsoids are shown at 50% probability.

dx.doi.org/10.1021/ic402208s | Inorg. Chem. 2013, 52, 13639–13643

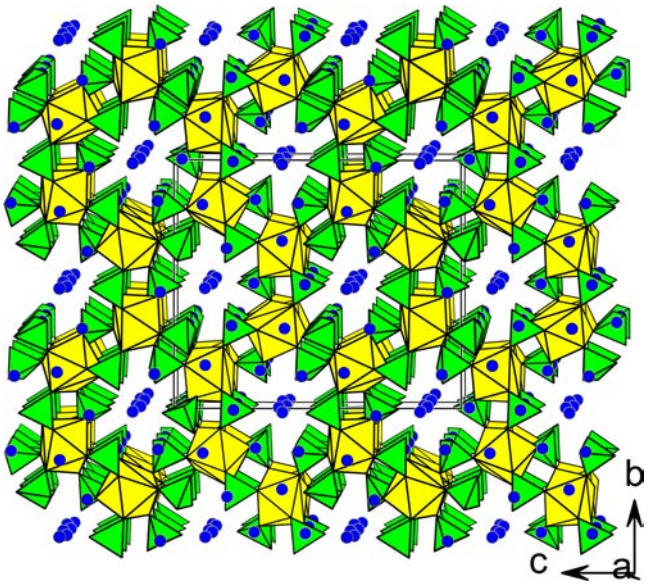

Figure 2. Structure of **1** viewed along the *a* axis. The yellow and green polyhedra are UO_8 dodecahedra and PO_4 tetrahedra, respectively. Blue circles represent Na atoms.

(Figure S4 of the Supporting Information). All 10 sodium sites are situated inside the channels and are fully occupied. Nevertheless, only Na(1) is located at the intersection of these perpendicular channels. The sodium atoms are coordinated by six, seven, eight, or nine oxygen atoms when the limiting value for the Na−O bond length, 3.19 Å, of Donnay and Allmann is considered.[23] The bond valence sum for Na(5) is 0.75, and those for other Na atoms range from 0.85 to 1.16. The significantly smaller valence sum and relatively larger thermal parameter for Na(5) indicate that the sodium atom is loosely bound. To check whether the Na(5) site is fully occupied, the multiplicity of Na(5) was allowed to be refined. Na(5) refined to a multiplicity of 1.00(1), indicating that the Na site is fully occupied.

Compound **2** is isotypic with **1**. Both Ce atoms are eight-coordinate with a geometry of snub disphenoid. Roulhac and Palenki reported that the average value of bond valence parameter R_o for a Ce−O bond length of 2.094 Å gave a good indication of whether the oxidation state of the Ce ion is +3 or +4 from the observed distances without any assumptions.[24] Bond valence sum calculations using the parameter give values of 3.99 and 4.02 valence units at Ce(1) and Ce(2) sites, respectively, consistent with the presence of Ce^{4+} ions in these sites. The sodium atoms are coordinated by six, seven, eight, or nine oxygen atoms. The bond valence sum for Na(5) is 0.73, and those for other Na atoms range from 0.86 to 1.14. The significantly smaller valence sum and relatively larger thermal parameter for Na(5) indicate that the sodium atom is loosely bound. The Na(5) site is fully occupied because the Na atom refined to a multiplicity of 1.00(1).

The structural chemistry of CePs is complex, but only a few have been structurally characterized. The first structures of CePs with P/Ce ratios of 1.5/1 and 2/1 have only recently been determined by powder X-ray diffraction. Two CePs with a P/Ce ratio of 3 have been reported, namely, $Ce(HPO_4)(H_2PO_4)_2{\cdot}2H_2O$ and $Na_5Ce(PO_4)_3$.[25,26] However, the crystal structures of these two compounds have remained unknown. $Na_5Ce(PO_4)_3$ was prepared under mild hydrothermal conditions in the pH range of 8−9 and was studied by elemental chemical analysis, powder XRD, IR, Raman, ^{31}P MAS NMR, and XPS spectroscopies. A comparison of the powder patterns of $Na_5Ce(PO_4)_3$ and compound **2** shows that they have the same structure. Using the high-temperature, high-pressure hydrothermal method, we have grown crystals of **2**. Its structure has been determined by single-crystal X-ray diffraction.

Spectroscopic Studies. As shown in Figure 3, transitions consistent with the U^{IV} valence state are observed in the solid-state UV−vis spectrum of **1**. The spectrum is similar to those of several U(IV) phosphates and phosphites.[27] The bands at 400−515, 515−560, and 580−700 nm are assigned to the transitions from the $^3H_4$ ground level to $^3P_2 + {}^1I_6$, $^3P_1$, and $^3P_0 + {}^1D_2 + {}^1G_4$ levels, respectively, according to the study of the absorption spectrum of U^{4+} in zircon ($ZrSiO_4$).[28] The structure of zircon also consists of eight-coordinate polyhedra (snub disphenoids). The strong band at 375 and shorter wavelengths are ascribed to $5f^2 \rightarrow 5f^16d^1$ transitions.

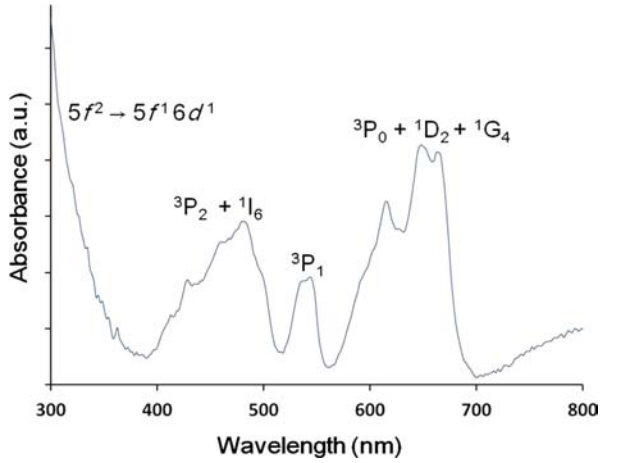

Figure 3. Room-temperature UV−vis absorption spectrum of **1**.

The U 4f XPS spectrum of **1** is shown in Figure 4, which was fit with one component and satellite peaks. The binding energies (BEs) of all peaks were referenced to the adventitious C 1s at 285 eV. The fitting parameters are listed in Table S1 of the Supporting Information. The primary peak positions are at 381.3 eV (U $4f_{7/2}$) and 392.2 eV (U $4f_{5/2}$), which are higher

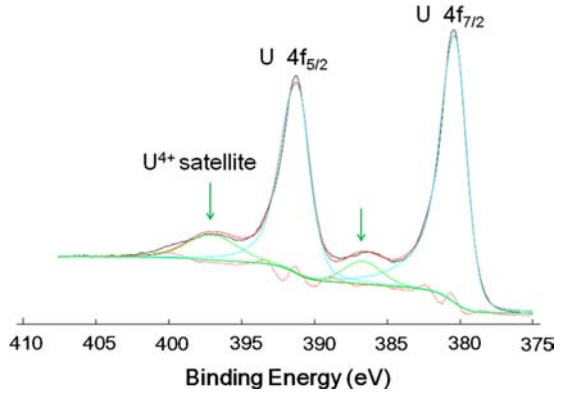

Figure 4. U 4f XPS spectrum of **1** (black line for data, red line for the fit envelope, blue line for main peaks, green line for satellites, and dotted line for the deviation).

dx.doi.org/10.1021/ic402208s | *Inorg. Chem.* 2013, 52, 13639−13643

than those of U^{4+} in $Cs_2USi_6O_{15}$ (379.7 and 390.5 eV, respectively),[7] $Cs_4UGe_8O_{20}$ (380.0 and 390.8 eV, respectively),[8] and $U(UO_2)(PO_4)_2$ (U $4f_{7/2}$, 380.7 eV),[27a] and comparable to that of U^{4+} in $H_8UMo_{12}O_{42}$ (U $4f_{7/2}$, 381.4 eV).[29] For uranium, both U 4f peaks show satellites at higher BEs: 6−7 eV for U^{4+}, 7.8−8.5 eV for U^{5+}, and 4 and 10 eV for U^{6+}.[30] The separations between the satellites and primary peaks for **1** are 6.4 and 6.1 eV, which are in good agreement with the values for U^{4+}. The XPS spectrum confirms the presence of U^{4+} in **1**.

In summary, we have synthesized and structurally characterized a new uranium(IV) phosphate that contains UO_8 snub-disphenoidal polyhedra. This is the first U(IV) phosphate synthesized under high-temperature, high-pressure hydrothermal conditions. The valence state of uranium was established by UV−vis and U 4f X-ray photoelectron spectroscopy. The isotypic Ce(IV) phosphate has also been synthesized and its crystal structure determined by single-crystal X-ray diffraction. It is the first structurally characterized Ce(IV) phosphate with a Ce/P ratio of 3. Both compounds are anhydrous, although they were synthesized in water. It has been reported that hydrothermal reaction under vigorous conditions prefers the formation of the anhydrous phase as compared with mild conditions.[31] The successful use of the hydrothermal method in the synthesis of these U(IV) and Ce(IV) phosphates suggests further opportunities for synthesizing more examples in these interesting classes of compounds. In the course of researching the synthesis of reduced uranium phosphates, we observed other phases whose dark color is indicative of mixed-valence compounds. Further research to synthesize reduced uranium phosphates and Ce(IV) phosphates and silicates is ongoing.

■ ASSOCIATED CONTENT

Supporting Information

X-ray crystallographic data of **1** and **2** in CIF format, PXRD patterns, and U 4f XPS fitting parameters. This material is available free of charge via the Internet at http://pubs.acs.org.

■ AUTHOR INFORMATION

Corresponding Author

*E-mail: liikh@cc.ncu.edu.tw.

Notes

The authors declare no competing financial interest.

■ ACKNOWLEDGMENTS

We thank the National Science Council of Taiwan for financial support, Ms. Meng-Ling Chen and Prof. Bor-Chen Chang at National Central University for SHG, and Ms. S.-L. Cheah at NTHU for XPS measurements.

■ REFERENCES

(1) Wang, Z.; Wang, S.; Ling, J.; Morrison, J. M.; Burns, P. C. *Inorg. Chem.* **2012**, *51*, 7185−7191.

(2) Finch, R.; Murakami, T. Systematics and Paragenesis of Uranium Minerals. In *Uranium: Mineralogy, Geochemistry and the Environment*; Burns, P. C., Finch, R., Eds.; Reviews in Mineralogy; Mineralogical Society of America: Chantilly, VA, 1999; Vol. *38*, pp 91−179.

(3) (a) Wang, X.; Huang, J.; Liu, L.; Jacobson, A. J. *J. Mater. Chem.* **2002**, *12*, 406−410. (b) Chen, C.-S.; Kao, H.-M.; Lii, K.-H. *Inorg. Chem.* **2005**, *44*, 935−940. (c) Lin, C.-H.; Chiang, R.-K.; Lii, K.-H. *J. Am. Chem. Soc.* **2009**, *131*, 2068−2069. (d) Ling, J.; Morrison, J. M.; Ward, M.; Poinsatte-Jones, K.; Burns, P. C. *Inorg. Chem.* **2010**, *49*, 7123−7128. (e) Morrison, J. M.; Moore-Shay, L. J.; Burns, P. C. *Inorg. Chem.* **2011**, *50*, 2272−2277.

(4) (a) Stieff, L. R.; Stern, T. W.; Sherwood, A. M. *Science* **1955**, *121*, 608−609. (b) Speer, J. A. *Rev. Mineral. Geochem.* **1980**, *5*, 113−135.

(5) Uvarova, Y. A.; Sokolova, E.; Hawthorne, F. C.; Agakhanov, A. A.; Pautov, L. A. *Can. Mineral.* **2004**, *42*, 1005−1011.

(6) Durif, P. A. *Acta Crystallogr.* **1956**, *9*, 533.

(7) Liu, H.-K.; Lii, K.-H. *Inorg. Chem.* **2011**, *50*, 5870−5872.

(8) Nguyen, Q. B.; Lii, K.-H. *Inorg. Chem.* **2011**, *50*, 9936−9938.

(9) Yudintsev, S. V.; Stefanovsky, S. V.; Ewing, R. C. Actinide Host Phases as Radioactive Waste Forms. In *Structural Chemistry of Inorganic Actinide Compounds*; Krivovichev, S. V., Burns, P. C., Tananaev, I. G., Eds.; Elsevier: Amsterdam, 2007; pp 457−490.

(10) Locock, A. J. Crystal Chemistry of Actinide Phosphates and Arsenates. In *Structural Chemistry of Inorganic Actinide Compounds*; Krivovichev, S. V., Burns, P. C., Tananaev, I. G., Eds.; Elsevier: Amsterdam, 2007; pp 217−278.

(11) Villa, E. M.; Marr, C. J.; Jouffret, L. J.; Alekseev, E. V.; Depmeier, W.; Albrecht-Schmitt, T. M. *Inorg. Chem.* **2012**, *51*, 6548−6558.

(12) Nazaraly, M.; Wallez, G.; Chaneac, C.; Tronc, E.; Ribot, F.; Quarton, M.; Jolivet, J.-P. *Angew. Chem., Int. Ed.* **2005**, *44*, 5691−5694 and references cited therein.

(13) Salvado, M. A.; Pertierra, P.; Trobajo, C.; Garcia, J. P. *J. Am. Chem. Soc.* **2007**, *129*, 10970−10971 and references cited therein.

(14) Sheldrick, G. M. *SAINT*, version 7.68A; University of Göttingen: Göttingen, Germany, 2009.

(15) Sheldrick, G. M. *SADABS*, version 2008/1; University of Göttingen: Göttingen, Germany, 2008.

(16) Sheldrick, G. M. *SHELXTL*, version 6.14; Bruker AXS GmbH: Karlsruhe, Germany, 2000.

(17) Sheldrick, G. M. *TWINABS*; University of Göttingen: Göttingen, Germany, 2008.

(18) Sheldrick, G. M. *cell_now*; University of Göttingen: Göttingen, Germany, 2008.

(19) Kurtz, S. K.; Perry, T. T. *J. Appl. Phys.* **1968**, *39*, 3798.

(20) Shannon, R. D. *Acta Crystallogr.* **1976**, *A32*, 751−767.

(21) Brese, N. E.; O'Keeffe, M. *Acta Crystallogr.* **1991**, *B47*, 192−197.

(22) Locock, A. J. In *Structural Chemistry of Inorganic Actinide Compounds*; Krivovichev, S. V., Burns, P. C., Tananaev, I. G., Eds.; Elsevier: Amsterdam, 2007; Chapter *6*, pp 217−278.

(23) Donnay, G.; Allmann, R. *Am. Mineral.* **1970**, *55*, 1003−1015.

(24) Roulhac, P.; Palenik, G. J. *Inorg. Chem.* **2003**, *42*, 118−121.

(25) Pajakoff, S. *Monatsh. Chem.* **1968**, *99*, 1400−1408.

(26) Xu, Y.-H.; Wang, D.; Feng, S.-H.; Pang, W.-Q.; Yue, Y. *Chem. Res. Chin. Univ.* **2000**, *16*, 287−300.

(27) (a) Bénard, P.; Louër, D.; Dacheux, N.; Brandel, V.; Genet, M. *Chem. Mater.* **1994**, *6*, 1049−1058. (b) Mandal, S.; Chandra, M.; Natarajan, S. *Inorg. Chem.* **2007**, *46*, 7935−7943. (c) Villa, E. M.; Marr, C. J.; Jouffret, F. J.; Alekseev, E. V.; Depmeier, W.; Albrecht-Schmitt, T. E. *Inorg. Chem.* **2012**, *51*, 6548−6558.

(28) Richman, I.; Kislink, P.; Wong, E. Y. *Phys. Rev.* **1967**, *155*, 262−267.

(29) (a) Tat'yanina, I. V.; Torchenkova, E. A.; Kazanskii, L. P.; Spitsyn, V. I. *Dokl. Akad. Nauk SSSR* **1977**, *234*, 1136. (b) Ilton, E. S.; Bagus, P. S. *Surf. Interface Anal.* **2011**, *43*, 1549−1560.

(30) Schindler, M.; Hawthorne, F. C.; Freund, M. S.; Burns, P. C. *Geochim. Cosmochim. Acta* **2009**, *73*, 2471−2478.

(31) Lii, K.-H.; Wen, N.-S.; Su, C.-C.; Chueh, B.-R. *Inorg. Chem.* **1992**, *31*, 439−442.